Environmental Science
Water Research & Technology

Kinetics and mechanism of hydrolysis of PF_6^- accelerated by H^+ or Al^{3+} in aqueous solution

Journal:	*Environmental Science: Water Research & Technology*
Manuscript ID	EW-ART-09-2024-000758.R1
Article Type:	Paper

Water Impact Statement

The challenge in hydrometallurgical recycling of lithium-ion batteries (LIBs) is the wastewater treatment containing LIBs electrolyte. $LiPF_6$ is most commonly used Li salt in LIBs, and the wastewater treatment of $LiPF_6$ is difficult due to its high stability in water. This study will help to design a more efficient process to treat wastewater containing $LiPF_6$.

Title

Kinetics and mechanism of hydrolysis of PF_6^- accelerated by H^+ or Al^{3+} in aqueous solution

Author names

Takuto Miyashita*, Kouji Yasuda* and Tetsuya Uda*

Department of Materials Science and Engineering, Graduate School of Engineering, Kyoto University, Kyoto, 606-8501, Japan.

*Corresponding authors

ORCID

Takuto Miyashita: https://orcid.org/0009-0009-9057-9215

Kouji Yasuda: https://orcid.org/0000-0001-5656-5359

Tetsuya Uda: https://orcid.org/0000-0002-2484-4297

Abstract

Treatment of wastewater containing PF_6^- is required during hydrometallurgical recycling of lithium-ion batteries. Because of the kinetic stability of PF_6^- in aqueous solution, the decomposition study into PO_4^{3-} or F^- is required for wastewater treatment. In our previous report, the hydrolysis of PF_6^- was shown to be accelerated by adding Al^{3+} and elevating the solution temperature. In this work, the kinetics and mechanism of the hydrolysis of PF_6^- at several pH and Al^{3+} concentrations were investigated for more efficient wastewater treatment. The solutions containing $LiPF_6$ at various pH and $AlCl_3$ concentrations were kept at 90 °C, and the concentration changes of PF_6^-, $PO_2F_2^-$, PO_3F^{2-}, PO_4^{3-}, and F^- were measured by ion chromatography. The measurement results were analyzed assuming pseudo-first-order kinetics. The results showed that Al^{3+} and H^+ accelerated the hydrolysis of $PO_2F_2^-$ and PO_3F^{2-}, but the levels of accelerating effects were different. More specifically, the accelerating effects of Al^{3+} are higher in the order of $PF_6^- > PO_2F_2^- > PO_3F^{2-}$, while the accelerating effects of H^+ are in the opposite order. Based on the discussion, a more efficient treatment process for wastewater containing PF_6^- was proposed. The proposed process is expected to reduce heating costs and processing time compared to previously reported ones.

1. Introduction

The safe disposal of spent lithium-ion batteries (LIBs) is required, with the increase of production of electric vehicles. The valuable metals need to be recovered from the spent LIBs as required by EU Battery Regulation,[1] and various recycling methods of LIBs are proposed.[2,3] In the initial step of the recycling, the spent LIBs are deactivated in some ways because LIBs pose ignition risk. The most commonly used deactivation method is heat treatment, so-called pyrometallurgical process. Another proposed process is hydrometallurgical process, in which spent LIBs are crushed in water at room temperature. The advantages of the hydrometallurgical process are lower energy costs and capital investment. After the deactivation on hydrometallurgical process, the black mass, which is a mixed powder of cathode and anode materials,

separator, current collectors, and cases are recovered as mixture of solids. It should be noted that the LIB electrolyte is dissolved in the water. The LIB electrolytes mainly contain carbonate ester as a solvent and lithium hexafluorophosphate ($LiPF_6$) as a lithium salt. In aqueous solutions, $LiPF_6$ dissociates into Li^+ and hexafluorophosphate ion (PF_6^-), and PF_6^- is kinetically stable at room temperature.[4] The treatment of wastewater containing phosphorus (P) and fluorine (F) is therefore an important problem.[5–7]

In general, P and F are removed from the industrial wastewater by precipitate formation *via* calcium hydroxide ($Ca(OH)_2$) addition, or coprecipitation with iron (III) or aluminum (III) hydroxide *via* pH adjustment after the addition of their trivalent salts.[8,9] To treat wastewater containing PF_6^- by these conventional treatments, the decomposition into PO_4^{3-} and F^- is necessary.[10] To accelerate the decomposition of PF_6^- in wastewater, the addition of strong acid[11–13] or aluminum (III) salts[10] at elevated temperatures have been proposed. To improve the efficiency of wastewater treatment, the investigation of the reaction rates and decomposition mechanism are required.

$LiPF_6$ is the most commonly used Li salt because of its stability at the operating temperature with the wide electrochemical window, high ionic conductivity, and solid-electrolyte interface (SEI) formation at both electrodes.[14] At room temperature, $LiPF_6$ is at least kinetically stable both in organic electrolyte and aqueous solutions. For instance, its concentration in 0.1 M $LiPF_6$ aqueous solution was almost constant at room temperature for more than 3 weeks.[4] In contrast, the hydrolysis proceeds when $LiPF_6$ is exposed to humid air in the powder form[15,16] or dissolved in the organic electrolytes containing trace amounts of water[17–19]. Particularly, there are many reports on the latter, as it may adversely affect the operation performance of LIBs. These typical reports show that the reaction of $LiPF_6$ with trace amounts of water in organic electrolytes proceeds according to the following reactions (1–5).

$$LiPF_6 \rightleftarrows PF_5 + LiF \quad (1)$$

$$PF_5 + H_2O \rightarrow POF_3 + 2\,HF \quad (2)$$

$$POF_3 + H_2O \rightarrow HPO_2F_2 + HF \quad (3)$$

$$HPO_2F_2 + H_2O \rightarrow H_2PO_3F + HF \quad (4)$$

$$H_2PO_3F + H_2O \rightarrow H_3PO_4 + HF \quad (5)$$

The intermediate products (PF_5, POF_3, HPO_2F_2, and H_2PO_3F) in reactions (1–5) were observed by ion chromatography[4,20], GC-MS[18,21], ESI-MS[20], and NMR[22].

Here, the attention should be paid that the hydrolysis proceeds in organic electrolytes with trace amounts of water but not in aqueous solutions. Based on the results of DFT and MD studies, Tasaki *et al.* pointed out that this difference may be due to the difference in the dissociation of $LiPF_6$ in the respective solvents.[23] The dissociation of $LiPF_6$ into Li^+ and PF_6^- (reaction (6)) is more promoted in water than carbonate solvents.

$$LiPF_6 \rightarrow Li^+ + PF_6^- \quad (6)$$

The kinetics of hydrolysis of PF_6^- in aqueous solution was reported under some conditions.[24,25] These reports showed that the hydrolysis was accelerated at lower pH or by cations such as Be^{2+}, Al^{3+}, Zr^{4+}, and Th^{4+}. The hydrolysis of the intermediates, $PO_2F_2^-$ and PO_3F^{2-}, was also reported under similar conditions.[26,27] These studies were conducted at only near room temperature and high acid concentration such as 2.0–10 mol L^{-1} (M) HCl solution. Furthermore, only the concentration of F^- was measured during the hydrolysis, and other products were not directly quantified.

In this study, the kinetics and mechanism on hydrolysis of PF_6^- and their intermediates were investigated in HCl acidic solution and Al^{3+}-containing solution at 90 °C. The hydrolysis behaviors were analyzed by ion chromatography to measure the concentration changes of anions accompanied by the hydrolysis. The pseudo-first-order rate constants were calculated, and the mechanism of accelerated hydrolysis was discussed. Based on the results of this study, an optimization of wastewater treatment was attempted.

2. Methods

Most of the solution preparation and analytical methods have been described in our previous report[10]. For solution preparation, $LiPF_6$ (Fujifilm Wako Pure Chemical Corporation, 98.0+ %), $AlCl_3 \cdot 6H_2O$ (Fujifilm Wako Pure Chemical Corporation., JIS Special Grade), HCl (Nacalai Tesque, INC., GR, 35 %), $LiPO_2F_2$ (Tokyo Chemical Industry Co., Ltd., > 98.0 %), Na_2PO_3F (Thermo Scientific Chemicals, 94 % min), and deionized water (DI, Organo Corporation, Pure Light, < 0.1 μS cm^{-1}) were used. To prevent the reaction with humidity, $LiPF_6$ was weighed in a glove box under an Ar atmosphere, and then transferred to air and mixed quickly with DI. The reagents were dissolved in DI to the desired composition. Then, 100 mL of the solutions were sealed in polypropylene screw containers and placed in a water bath (As One Corporation, HWA-50A) kept at 90 °C. The solution pH was measured by pH electrode (Horiba, Ltd., 9632-10D) calibrated according to National Institute of Standard and Technology (NIST) standards. The anion concentrations were quantified by ion chromatography (Shimadzu Corporation, HIC-ESP, column: Shim-pack IC-SA2, suppressor: ICDS-40A, electrical conductivity detector: CDD-10AVP). The eluent of 3.6 mM Na_2CO_3 (Fujifilm Wako Pure Chemical Corporation., JIS Special Grade) + 3.4 mM $NaHCO_3$ (Fujifilm Wako Pure Chemical Corporation., JIS Special Grade) was flowed at 1.0 mL min^{-1} through the column kept at 50 °C. The solutions to be measured were injected by an autosampler (Shimadzu Corporation, SIL-20A). The concentrations of PF_6^-, $PO_2F_2^-$, PO_3F^{2-}, PO_4^{3-}, and F^- were measured. Standard solutions were prepared by dissolving $LiPF_6$, $LiPO_2F_2$, Na_2PO_3F, 1000 ppm PO_4^{3-} standard solution (Fujifilm Wako Pure Chemical Corporation, Japan Calibration Service System (JCSS)), and 1000 ppm F^- standard solution (Fujifilm Wako Pure Chemical Corporation, JCSS) into DI. By measuring three or more concentrations for each standard solution and concentration range, calibration curves were derived as shown in Figs. S1 and S2. It is noted that acid dissociation states are not distinguishable by ion chromatography, so these chemical species are described as fully dissociated state (such as $PO_2F_2^-$, PO_3F^{2-}, PO_4^{3-}, and F^-) except for the section discussing acid dissociation states.

In the investigation for the effect of various cations, $Al_2(SO_4)_3 \cdot 14–18H_2O$ (Kanto Chemical Co., Inc., GR), $Cr_2(SO_4)_3 \cdot xH_2O$ (Fujifilm Wako Pure Chemical Corporation, 99.5 %), Y_2O_3 (Nippon Yttrium

Co., Ltd., 99.99 %), $Ce_2(SO_4)_3 \cdot nH_2O$ (Fujifilm Wako Pure Chemical Corporation, 99.5 %), La_2O_3 (Nacalai Tesque, Inc., GR, ≧ 99.99 %), MgO (Wako Pure Chemical Corporation, 99.9 %), CuO (Nacalai Tesque, Inc., GR), and $Ca(OH)_2$ (Nacalai Tesque, Inc., GR) were used. Eight solutions of 10 mM $LiPF_6$ with each cation at concentration of 2 mM were prepared. The initial pH of the solutions was adjusted to 3.8–4.0 by adding HCl or NaOH solutions After keeping at 90 °C for 24 hours, the concentration of F^- was measured by fluoride-ion selective electrode (HORIBA, Ltd., 6561S-10C).

3. Results

3.1. Concentration changes of anions during the hydrolysis of PF_6^- in acidic solution at 90 °C

To investigate the effect of pH on the hydrolysis, three different solutions of 10 mM $LiPF_6$ were prepared, with initial pH 2.5 (exp. #01), 1.8 (exp. #02), and 1.1 (exp. #03), respectively. The solution pH was adjusted by adding HCl solution. The solutions were kept at 90 °C, and the changes of each anion concentration and pH were measured as shown in Fig. 1. For exp. #01–03, the concentration of PF_6^- decreases, and $PO_2F_2^-$, PO_3F^{2-}, PO_4^{3-}, and F^- are produced over time. The sum amounts of P and F of these anions are constantly about 10 mM and 60 mM, respectively. This suggests that unexpected compounds containing P and F are not stable. The concentrations of PO_4^{3-} and F^- increase for all conditions. Meanwhile, the concentrations of $PO_2F_2^-$ and PO_3F^{2-} increase initially and then decrease. This indicates that $PO_2F_2^-$ and PO_3F^{2-} are produced as intermediate products, and PO_4^{3-} and F^- are produced as final products. As indicated by the scales of the horizontal axis of each graph, the hydrolysis of PF_6^- is accelerated at lower pH; the half-life of PF_6^- is approximately 35 hours, 10 hours, and 2–3 hours for initial pH 2.5 (exp. #01), 1.8 (exp. #02), and 1.1 (exp. #03), respectively. The hydrolysis of $PO_2F_2^-$ and PO_3F^{2-} is also faster at lower initial pH. During the hydrolysis, the pH decreases in exp. #01 and increases in exp. #02 and #03. The behaviors of $PO_2F_2^-$ and PO_3F^{2-} and pH changes are discussed later.

*** Figure 1 ***

3.2. Concentration changes of anions during the hydrolysis of PF_6^- with Al^{3+} at 90 °C

The effects of Al^{3+} on the hydrolysis were investigated. Two different solutions of 10 mM $LiPF_6$ with 10 mM $AlCl_3$ (exp. #04) and 100 mM $AlCl_3$ (exp. #05) were prepared, respectively. The solutions were kept at 90 °C, and the reaction was analyzed. The measurement results of each anion concentration and pH are shown in Fig. 2. The initial pH values of prepared solutions of exp. #04 and #05 are 3.5 and 3.1, respectively. The half-lives of PF_6^- are in the range of 1–2 hours and 0–0.5 hours for 10 mM $AlCl_3$ (exp. #04) and 100 mM $AlCl_3$ (exp. #05), respectively. Compared to the half-life of 35 hours for exp. #01 with an initial pH of 2.5, the hydrolysis of PF_6^- is much faster with $AlCl_3$ addition, despite the relatively high initial pH. The concentrations of $PO_2F_2^-$ and PO_3F^{2-} follow a similar trend to acidic solutions, increasing initially and then decreasing. As the hydrolysis reaction proceeds, the pH decreases to 1.6 and 1.3 for exp. #04 and #05, respectively. The behaviors of $PO_2F_2^-$, PO_3F^{2-}, and pH are discussed later. In another experiment, the effect of anion in aluminum salts ($AlCl_3$, $Al_2(SO_4)_3$, and $Al(NO_3)_3$) on hydrolysis was

examined, and the details were discussed in Fig. S3. The anions affected the hydrolysis rates, but the effect was very small compared to the accelerating effect of Al^{3+}.

*** Figure 2 ***

3.3. Measurement of the hydrolysis of $PO_2F_2^-$ and PO_3F^{2-} at several conditions

The effects of pH and Al^{3+} on the hydrolysis of $PO_2F_2^-$ and PO_3F^{2-} were investigated. Four different solutions of 10 mM $LiPO_2F_2$ with each level of pH and $AlCl_3$ were prepared and kept at 90 °C; pH 3.1 without $AlCl_3$ (exp. #06), pH 1.0 without $AlCl_3$ (exp. #07), pH 3.0 with 100 mM $AlCl_3$ (exp. #08), and pH 1.0 with 100 mM $AlCl_3$ (exp. #09). The concentration changes of $PO_2F_2^-$ are shown in Fig. 3. The hydrolysis percentages at initial pH 3.0–3.1 for 0.5 hours are more than 40 % with Al^{3+} (exp. #08) but negligible without Al^{3+} (exp. #06). On the other hand, regardless of the presence of Al^{3+}, more than 80 % of $PO_2F_2^-$ is decomposed within 0.5 hours at pH 1.0 (exp. #07 and #09).

The hydrolysis of PO_3F^- at 90 °C was also investigated under similar conditions; pH 2.7 without $AlCl_3$ (exp. #10), pH 1.0 without $AlCl_3$ (exp. #11), pH 2.4 with 100 mM $AlCl_3$ (exp. #12), and pH 1.0 with 100 mM $AlCl_3$ (exp. #13). The concentration changes of PO_3F^- are shown in Fig. 4. The hydrolysis of PO_3F^{2-} is very slow at pH 2.4–2.7 regardless of the presence of Al^{3+} (exp. #10, 12). However, at pH 1.0 without Al^{3+} (exp. #11), more than 95 % of PO_3F^{2-} are decomposed within 30 min. Here, it should be noted that the hydrolysis of PO_3F^{2-} is rather suppressed at pH 1.0 by adding Al^{3+} (exp. #13), which is different from the behavior for PF_6^- and $PO_2F_2^-$. The kinetics and mechanism of these hydrolysis are discussed later.

*** Figure 3 ***

*** Figure 4 ***

4. Discussion

4.1. Chemical equilibrium of the products of the hydrolysis

4.1.1 Stable species in phosphate-fluoride system in aqueous solution

The hydrolysis of PF_6^- and its intermediate products $PO_2F_2^-$ and PO_3F^{2-} is discussed in detail. First, equilibrium calculation was conducted to determine if the reverse reactions could be disregarded for kinetic analysis. The equilibrium state of each chemical species in an aqueous solution was calculated by the standard Gibbs energy of formation.[28,29] There is no report on standard Gibbs energy of formation of PF_6^- as far as we know, so the equilibrium calculation was conducted without considering PF_6^-. The conditions of calculation are 10 mM for PO_4^{3-} and 60 mM for F^-, assuming the complete hydrolysis of 10 mM PF_6^-. The equilibrium calculation was conducted on PHREEQC version 2 released by U.S. Geological Survey.[30] The calculated equilibrium concentration of each chemical species is shown in Fig. 5. In the pH range of 1–4 which is the target of this study, the stable acid dissociation states of HPO_2F_2, H_2PO_3F, H_3PO_4, and HF are $PO_2F_2^-$, HPO_3F^-, H_3PO_4 (or $H_2PO_4^-$), and HF, respectively. Comparing the stability of these chemical species, H_3PO_4 (or $H_2PO_4^-$) is more stable than $PO_2F_2^-$ and HPO_3F^- with a difference in concentration of about 10^2 and 10^8, respectively. Therefore, in the hydrolysis of $PO_2F_2^-$ and HPO_3F^-, the reverse reaction

can be assumed to be negligibly slow in contrast to the forward reaction. Although there is no clear evidence for the hydrolysis of PF_6^-, the reverse reaction of the hydrolysis reactions assumed to be negligibly slow. Therefore, only the forward reactions are considered in the following discussion of kinetics.

*** Figure 5 ***

4.1.2. Changes of pH accompanying the hydrolysis

Second, the changes of pH accompanying hydrolysis are discussed from the viewpoint of chemical equilibrium. The values of acid dissociation constant (pK_a) for HPF_6, HPO_2F_2, H_2PO_3F, H_3PO_4, and HF are shown in Table 1.[28,29,31] Note that the value for PF_6^- is unreliable due to lack of the original data in literature sources[31]. Considering the majority states of the anions from the values of pK_a, the hydrolysis reactions in the pH range of 2.5–2.2 in exp. #01 can be described as reactions (7–9).

pH range of 2.5–2.2

$$PF_6^- + 2\ H_2O \rightarrow PO_2F_2^- + 4\ HF \quad (7)$$

$$PO_2F_2^- + H_2O \rightarrow HPO_3F^- + HF \quad (8)$$

$$HPO_3F^- + H_2O \rightarrow H_2PO_4^- + HF \quad (9)$$

The concentration of H^+ does not change with reactions (7–9), and the solution pH is expected to be constant. On the other hand, the initial pH in exp. #02 and #03 (about 1.8 and 1.1, respectively) was below the value of pKa_1 of phosphoric acid (= 2.148). At solution pH below the pKa_1, the stable state of phosphoric acid is expected to be H_3PO_4. Therefore, reaction (9) is replaced by reaction (10).

pH range below pKa_1 of phosphoric acid (= 2.148)

$$HPO_3F^- + H_2O + H^+ \rightarrow H_3PO_4 + HF \quad (10)$$

The solution pH is expected to increase toward 2.148 depending on the consumption amount of H^+ in reaction (10).

Here, there were some differences between theoretical and experimental results as described below. During the hydrolysis in exp. #02, the pH exceeded 2.148 and increased to 2.6. Also, in exp. #03, the pH increased to 2.0 beyond the amount of H^+ consumed in reaction (10); the necessary amount of H^+ for pH increase from 1.1 to 2.0 is around 70 mM, but the amount of consumed H^+ by the reaction is around 8 mM. The reason for this rapid increase of pH during the reaction was probably due to the effect of HF on the pH electrode produced by hydrolysis. In fact, the simulated test showed that the indicated value by the pH electrode increased when HF was present in the solution. Exceptionally, the indicated value by the pH electrode remained stable when both Al^{3+} and HF are present (see Fig. S4).

*** Table 1 ***

Third, the pH decreases during the hydrolysis of PF_6^- in the solution containing Al^{3+} is discussed. In exp. #04 (10 mM $AlCl_3$) and #05 (100mM $AlCl_3$), pH decreased from 3.5 to 1.6 and from 3.1 to 1.3, respectively. The main reason for pH decrease is expected to be the formation of aluminum fluoride complexes according to reaction (11). The value of n in reaction (11) depends on the concentrations of Al^{3+} and F^-. For example, the equilibrium species at the initial concentration of 100 mM Al^{3+} and 60 mM F^- are shown in Fig. 6. In this condition, AlF^{2+} is the most stable fluoride complex below pH 3.

$$Al^{3+} + n\ HF \rightarrow AlF_n^{(3-n)+} + n\ H^+ \qquad (11)$$
$$n = 1–6$$

*** Figure 6 ***

4.2. Kinetics and mechanism of hydrolysis

4.2.1 Hydrolysis of PF_6^-

The hydrolysis rates of PF_6^- were quantitatively evaluated from the results shown in Figs. 1 and 2. The hydrolysis of PF_6^- was reported to experimentally follow pseudo-first-order kinetics as expressed in eqn. (12),[24,25]

$$-\frac{d[PF_6^-]}{dt} = k_{obs}\,[PF_6^-] \qquad (12),$$

in which $[PF_6^-]$ stands for the concentration of PF_6^- at reaction time t, and k_{obs} is the pseudo-first-order rate constant. Further discussion might be necessary on the elemental reactions, but it is reasonable to assume that the hydrolysis is a first-order reaction with a constant H^+ concentration based on past experimental evidence. Since the purpose of this study is to derive numerical data for estimating industrial processing rates for optimal treatments, the evaluation is conducted as pseudo-first-order kinetics on the basis of the past study. When the hydrolysis rate of PF_6^- follows eqn. (12), eqns. (13, 14) are valid:

$$[PF_6^-] = [PF_6^-]_0 \exp(-k_{obs}\,t) \qquad (13)$$

$$-\ln\left(\frac{[PF_6^-]}{[PF_6^-]_0}\right) = k_{obs}\,t \qquad (14),$$

in which $[PF_6^-]_0$ is the concentration of PF_6^- before the reaction. Thus, the observed pseudo-first-order reaction rate constant, k_{obs}, is obtained as the slope of $-\ln\left(\frac{[PF_6^-]}{[PF_6^-]_0}\right)$ plotted against reaction time t.

The experimental values of $-\ln\left(\frac{[PF_6^-]}{[PF_6^-]_0}\right)$ against reaction time t are plotted for different pH (exp. #01–03) and Al^{3+} concentrations (exp. #04–05) as shown in Fig. 7, respectively. The values of k_{obs} were

calculated using the least-squares method through the origin and listed in Table 2. The reasons for the large fitting deviation and standard error in exp. #04 are discussed later.

*** Figure 7 ***

*** Table 2 ***

The values of k_{obs} show that the hydrolysis of PF_6^- is accelerated at higher acid concentrations or with an addition of Al^{3+}. In particular, when Al^{3+} is added, the rate constants significantly increase by 1–2 orders of magnitude. Previous study also reported the values of k_{obs} at around room temperature as shown in Table 3.[24-26] In these reports, the ranges of temperature and acid concentration were limited to 25–45 °C, and 1.0–2.0 M in most cases, respectively, but the dependence of hydrolysis rate on pH or cation addition followed similar trend in this study. A notable aspect of the comparison between previous reports and this study is the accelerating effect of heating. In the previous report, the value of k_{obs} was 0.0764×10^{-4} in 1 M HCl at 25 °C (equivalent to pH 0) in Table 3(a). In contrast, at pH 1 and 90 °C (exp. #03 of this study), the value of k_{obs} was 48.2×10^{-4}, which is approximately 600 times faster, despite the relatively high pH.

*** Table 3 ***

The acceleration of hydrolysis by cations was reported to result from the hard acid–hard base interaction.[25] The cations such as H^+ and Al^{3+} have high affinity with F^-. The PF_6^- anion is subjected to electrophilic attack by these cations, and F atoms and an electron pair are transferred from PF_6^- to the cations according to reaction (15),

$$PF_6^- + 4\ M^{n+} + 2\ H_2O \rightarrow PO_2F_2^- + 4\ MF^{(n-1)+} + 4\ H^+ \quad (15),$$

in which $M^{n+} = H^+$ or Al^{3+}.

To support this discussion, the relationship between the hydrolysis rate and the affinity of added cation with F^- was studied. The formation constant (log K) of fluoride complex for each cation ($M^{n+} + F^- \rightarrow MF^{(n-1)+}$) was obtained from the NIST SRD 46 databese.[32] The studied cations in this study are M^{n+} = Al^{3+}, Cr^{3+}, Y^{3+}, Ce^{3+}, La^{3+}, Mg^{2+}, Cu^{2+}, and Ca^{2+}. These cations were selected because of relatively high log K and enough high solubilities of their hydroxide at around pH 4. The effects of these cations in accelerating hydrolysis of PF_6^- were examined by measuring F^- concentration after keeping 10 mM $LiPF_6$ solutions with respective cations at 90 °C for 24 hours. When analyzing F^- concentration, by adding total ionic strength adjustment buffer (TISAB) solution, F^- coordinated cations as $MF^{(n-1)+}$ are dissociated by chelating effect and quantified as F^-.[10] The relationship between the value of Log K and the concentration of F^- for the addition of each cation is plotted in Fig. 8. Positive correlation indicates that the hydrolysis of PF_6^- is accelerated by cation which has higher affinity with F^-. This result supports that the hydrolysis of PF_6^- proceeds through electrophilic attack by such cation. It should be added that the log K of Li^+ is relatively small (log K = 0.23), and the accelerating effect of Li^+ is expected to be small.

Here, the complex formation constant of AlF^{2+} (log K = 7) is higher than that of HF (log K = 3.17), and Al^{3+} is expected to be more effective than H^+ in accelerating the hydrolysis of PF_6^-. This is consistent with experimental results in this work. In addition, the reasons for the large fitting deviation and standard error in exp. #04 as shown in Fig.7 can be explained by the formation of aluminum fluoride complexes. Aluminum fluoride complexes such as AlF^{2+} exhibit less affinity with F^- than Al^{3+} and thus have a weaker accelerating effect on hydrolysis of PF_6^-. In exp. #04, the concentration of added Al^{3+} is only 10 mM, and the aluminum fluoride complexes increase and Al^{3+} decreases with the progress of hydrolysis, resulting in a lower hydrolysis rate.

*** Figure 8 ***

4.2.2 Hydrolysis of $PO_2F_2^-$ and PO_3F^{2-}

The hydrolysis of $PO_2F_2^-$ and PO_3F^{2-} is also reported to follow pseudo-first-order kinetics, as expressed in eqns. (16, 17).[26,27]

$$[PO_2F_2^-] = [PO_2F_2^-]_0 \exp(-k_{obs}\, t) \quad (16)$$

$$[PO_3F^{2-}] = [PO_3F^{2-}]_0 \exp(-k_{obs}\, t) \quad (17)$$

The hydrolysis of $PO_2F_2^-$ and PO_3F^{2-} in Figs.3 and 4 was evaluated on the assumption that it follows pseudo-first-order kinetics. The experimental values of $-\ln\left(\frac{[PO_2F_2^-]}{[PO_2F_2^-]_0}\right)$ in exp. #06–09 and $-\ln\left(\frac{[PO_3F^{2-}]}{[PO_3F^{2-}]_0}\right)$ in exp. 10–13 against reaction time t are plotted in Fig. 9. The values of k_{obs} calculated from the concentrations of $PO_2F_2^-$ or PO_3F^{2-} in exp. #06–13 were listed in Table 4. In #06 and #10, the standard errors for the value of k_{obs} are large, which is expected due to the greater influence of measurement error in the case of slow decomposition and small concentration changes. The values of k_{obs} in Table 4 indicate that the addition of Al^{3+} or decrease of pH accelerates the hydrolysis rates of $PO_2F_2^-$ and PO_3F^{2-}as well as the hydrolysis of PF_6^-.

Here, the H^+ concentration at around pH 1 is almost equal to 100 mM, and therefore, the accelerating effects can be compared between H^+ and Al^{3+} using the rate constants of the hydrolysis at pH 1.0–1.1 without Al^{3+} (exp. #03, #07, and #11) and at pH 2.4–3.1 with 100 mM Al^{3+} (exp. #05, #08, and #12). The values of k_{obs} were compared among these experiments results as shown in Fig. 10. Clearly, the accelerating effects of Al^{3+} are higher in the order of $PF_6^- > PO_2F_2^- > PO_3F^{2-}$, while the accelerating effects of H^+ are in the opposite order. The hydrolysis of PF_6^- is more accelerated by Al^{3+} than H^+, and the hydrolysis of $PO_2F_2^-$ and PO_3F^{2-} is more accelerated by H^+. It is also noteworthy and very unique feature that under low pH such as pH 1 (exp. #11 and #13) in Table 4, the addition of Al^{3+} does not accelerate the hydrolysis of PO_3F^{2-}, but rather suppresses it to one-eighth rate. This discussion explains the results that when PF_6^- is decomposed at pH 1.1 in Fig. 1 (c) (exp. #03), little $PO_2F_2^-$ and PO_3F^{2-} are detected, whereas when PF_6^- is decomposed with 100 mM $AlCl_3$ in Fig. 2 (b) (exp. #05), the concentrations of $PO_2F_2^-$ and PO_3F^{2-} are temporarily higher. The previously reported values of k_{obs} are shown in Table 3. The hydrolysis

of $PO_2F_2^-$ and PO_3F^{2-} is accelerated at higher acid concentrations and/or higher temperatures. The addition of Zr^{4+} suppresses hydrolysis of PO_3F^{2-} at high acid concentration such as 1.0 M HCl. The results in this work show the same trends in the previous work despite the different conditions of temperature and concentration. These phenomena cannot yet be fully explained. The coordination states may affect the rate of the hydrolysis, and further investigations such as first-principles calculations and spectroscopic measurements are needed.

*** Figure 9 ***

*** Table 4 ***

*** Figure 10 ***

4.3. Optimization of wastewater treatment

Based on the results in this study, a more efficient treatment process for wastewater containing PF_6^- is proposed. The previously reported process involves the hydrolysis step of PF_6^- to PO_4^{3-} and F^- by adding Al^{3+} or H^+, followed by the precipitation removal of PO_4^{3-} and F^- by adding $Ca(OH)_2$.[10] In this study, the detail of hydrolysis is investigated, and the results show that Al^{3+} is favorable for accelerating the hydrolysis of PF_6^-, but the hydrolysis of $PO_2F_2^-$ and PO_3F^{2-} rate-determining step as seen in Fig. 2 (b). Here, in the alkaline solution, $PO_2F_2^-$ and PO_3F^{2-} were reported to be decomposed rapidly.[26] The hydrolysis of $PO_2F_2^-$ and PO_3F^{2-} under acidic conditions was accelerated by the catalytic action of H^+ whereas $PO_2F_2^-$ and PO_3F^{2-} are thermodynamically unstable in alkaline solutions. Note that PF_6^- is kinetically very stable even in alkaline solutions. In saturated $Ca(OH)_2$ solution at pH 12, $PO_2F_2^-$ is completely decomposed in 1 hour, but the decomposition of PO_3F^{2-} is relatively slow; 40 % decomposition in 1 hour as shown in Fig. S5. Therefore, in the hydrolysis step with Al^{3+} at elevated temperature, the heating time can be shortened so that only PF_6^- is sufficiently decomposed. The remaining $PO_2F_2^-$ and PO_3F^{2-} are decomposed in the subsequent precipitation step by adding $Ca(OH)_2$ since the solution becomes alkaline.

Fig. 11 shows the flowchart of the proposed process to reduce heating costs and processing time and the results of the analysis at each step in the experimental verification. In this experiment, the solution of 10 mM $LiPF_6$ + 100 mM $AlCl_3$ (solution 1 in Fig.11) was prepared and kept at 90 °C for 1 hour (solution 2). Then, 432 mM $Ca(OH)_2$ was added to the solution, and precipitate was formed. After the solution was kept at room temperature for 1 hour, the supernatant (solution 3) and precipitate were separated. The quantification by ion chromatography shows that more than 95 % of PF_6^- were decomposed into $PO_2F_2^-$, PO_3F^{2-}, PO_4^{3-}, and F^- by heating at 90 °C for 1 hour. After the precipitation step, the all concentrations of $PO_2F_2^-$, PO_3F^{2-}, PO_4^{3-}, and F^- decreased to less than 0.6 mM. This result shows that not only PO_4^{3-} and F^- but also $PO_2F_2^-$ and PO_3F^{2-} are removed during precipitation step with $Ca(OH)_2$ addition. The XRD pattern of the precipitate showed $Ca_2AlClO_3(H_2O)_5$, a type of layered double hydroxide (LDH)[33] as shown in Fig. S7, which is reported to have the ability to remove the anions in the solution by ion exchange. It is noted that PO_3F^{2-} is removed almost completely in 1 hour (Fig. 11(b), Solution 3). The comparison with the

slower decomposition of PO_3F^{2-} in Fig. S5 suggests that PO_3F^{2-} is removed by the ion exchange of the LDH precipitate. Such type of removal by ion exchange ability was observed in our previous repor.[10]

*** Figure 11 ***

5. Conclusion

In this work, the kinetics and mechanism of hydrolysis of PF_6^- were investigated. The concentration changes of anions (PF_6^-, $PO_2F_2^-$, PO_3F^{2-}, PO_4^{3-}, and F^-) in the solutions of 10 mM $LiPF_6$ at various pH with various concentrations of $AlCl_3$ were measured during the keeping at 90 °C. Without Al^{3+}, the half-lives of PF_6^- were approximately 35 hours, 10 hours, and 2–3 hours for initial pH 2.5 (exp. #01), 1.8 (exp. #02), and 1.1 (exp. #03), respectively. With Al^{3+}, the half-lives of PF_6^- were in the range of 1–2 hours and 0–0.5 hours for 10 mM $AlCl_3$ (exp. #04) and 100 mM $AlCl_3$ (exp. #05), respectively. Compared to the half-life of 35 hours for exp. #01 with an initial pH of 2.5, the hydrolysis of PF_6^- is much faster with $AlCl_3$ addition, despite the relatively high initial pH. These results were analyzed as following pseudo-first-order kinetics. When comparing the effects of H^+ (pH 1.0–1.1 without Al^{3+} for exp. #03) and Al^{3+} (pH 2.4–3.1 with 100 mM Al^{3+} for exp. #05), the rate constant for hydrolysis of PF_6^- is greater for Al^{3+} than H^+. This indicates that the hydrolysis of PF_6^- is accelerated by Al^{3+} than H^+. The effects of Al^{3+} and pH on the hydrolysis of $PO_2F_2^-$ and PO_3F^{2-} were also individually investigated. The results showed that Al^{3+} and H^+ accelerated the hydrolysis of $PO_2F_2^-$ and PO_3F^{2-}, but the levels of accelerating effects were different. More specifically, the accelerating effects of Al^{3+} are higher in the order of $PF_6^- > PO_2F_2^- > PO_3F^{2-}$, while the accelerating effects of H^+ are in the opposite order. The hydrolysis of PF_6^- is more accelerated by Al^{3+} than H^+, and the hydrolysis of $PO_2F_2^-$ and PO_3F^{2-} is more accelerated by H^+. As a result, when considering the hydrolysis from PF_6^- to the final product PO_4^{3-} in strong acid solution without Al^{3+}, PF_6^- is decomposed relatively slowly, but $PO_2F_2^-$ and PO_3F^{2-} are decomposed relatively quickly. Conversely, in solution with Al^{3+}, PF_6^- is decomposed relatively quickly, and the hydrolysis of $PO_2F_2^-$ and PO_3F^{2-} is rate-determining step.

For wastewater treatment, an efficient process was proposed based on these results. In conventional process, PF_6^- is decomposed into PO_4^{3-} and F^- in strong acid solution by heating, followed by the precipitation removal of PO_4^{3-} and F^- by adding $Ca(OH)_2$. In our proposed process, the heating time of decomposition step is reduced. At elevated temperature, PF_6^- is quickly decomposed by adding Al^{3+}, but $PO_2F_2^-$ and PO_3F^{2-} remains in the solution. Then, by adding $Ca(OH)_2$, the solution becomes alkaline and the precipitate of LDH is formed, where $PO_2F_2^-$ is decomposed and PO_3F^{2-}, PO_4^{3-}, and F^- are precipitated by ion exchange of LDH. The simulated experiment demonstrated that reduction in processing time was feasible. This study will greatly contribute to the design of more efficient processes for the treatment of wastewater containing PF_6^-.

Author contributions

All authors conceived the ideas. T. M. contributed to the execution of the experiments, wrote the manuscript, and performed the analysis. All authors reviewed the manuscript.

Conflicts of interest

The authors have filed a patent covering the process described in this manuscript to Japanese Patent Application. Patent applicant: Kyoto University. Name of inventors: Takuto Miyashita, Kouji Yasuda and Tetsuya Uda. Application number: 2024-106337.

Acknowledgments

This work was financially supported by JX Advanced Metals Corporation. This work was also supported by the Adaptable and Seamless Technology transfer Program through Target-driven R&D (A-STEP), Grant Number JPMJTR20TF from Japan Science and Technology Agency (JST), and the establishment of university fellowships towards the creation of science technology innovation, Grant Number JPMJFS2123 from JST. This work was conducted as collaboration research of the Laboratory of Design of Sustainable Materials and Processing and the Laboratory of Non-ferrous Extractive Metallurgy, Department of Materials Science and Engineering, Graduate School of Engineering, Kyoto University. The Laboratory of Non-ferrous Extractive Metallurgy is an endowed chair by Mitsubishi Material Corp. We would like to acknowledge Dr. Takumi Yasuda, Dr. Akihiro Kishimoto at Kyoto University, and Prof. Takashi Nakamura at Tohoku University for fruitful discussion. This paper is part of the doctoral dissertation of Takuto Miyashita.

References

1 European Union Law, *REGULATION (EU) 2023/1542 OF THE EUROPEAN PARLIAMENT AND OF THE COUNCIL of 12 July 2023 concerning batteries and waste batteries*.

2 Z. J. Baum, R. E. Bird, X. Yu and J. Ma, Lithium-ion battery recycling─overview of techniques and trends, *ACS Energy Lett.*, 2022, **7**, 712–719.

3 D. L. Thompson, J. M. Hartley, S. M. Lambert, M. Shiref, G. D. J. Harper, E. Kendrick, P. Anderson, K. S. Ryder, L. Gaines and A. P. Abbott, The importance of design in lithium ion battery recycling – a critical review, *Green Chemistry*, 2020, **22**, 7585–7603.

4 M. Stich, M. Göttlinger, M. Kurniawan, U. Schmidt and A. Bund, Hydrolysis of $LiPF_6$ in carbonate-based electrolytes for lithium-ion batteries and in aqueous media, *J. Phys. Chem. C*, 2018, **122**, 8836–8842.

5 T. Uda, A. Kishimoto, K. Yasuda and Y. Taninouchi, Submerged comminution of lithium-ion batteries in water in inert atmosphere for safe recycling, *Energy Advances*, 2022, **1**, 935–940.

6 T. Fujita, H. Chen, K. Wang, C. He, Y. Wang, G. Dodbiba and Y. Wei, Reduction, reuse and recycle of spent Li-ion batteries for automobiles: A review, *Int J. Miner. Metall. Mater.*, 2021, **28**, 179–192.

7 E. Mossali, N. Picone, L. Gentilini, O. Rodrìguez, J. M. Pérez and M. Colledani, Lithium-ion batteries towards circular economy: A literature review of opportunities and issues of recycling treatments, *Journal of Environmental Management*, 2020, **264**, 110500.

8 J. T. Bunce, E. Ndam, I. D. Ofiteru, A. Moore and D. W. Graham, A review of phosphorus removal technologies and their applicability to small-scale domestic wastewater treatment systems, *Front. Environ. Sci.*, 2018, **6**, 8.

9 C. F. Z. Lacson, M.-C. Lu and Y.-H. Huang, Fluoride-containing water: A global perspective and a pursuit to sustainable water defluoridation management -An overview, *Journal of Cleaner Production*, 2021, **280**, 124236.

10 T. Miyashita, K. Yasuda and T. Uda, Removal of phosphorus and fluorine from wastewater containing PF_6^- *via* accelerated decomposition by Al^{3+} and chemical precipitation for hydrometallurgical recycling of lithium-ion batteries, *Environ. Sci.: Water Res. Technol.*, 2024, **10**, 1245–1255.

11 T. Mitsui, H. Kawamoto, J. Kamiya, *WO Pat.*, WO2013054875, 2013.

12 Y. Mochida, *JP Pat.*, JP1994170380, 1994.

13 H. Kikuyama, M. Miyashita and T. Fukudome, *WO Pat.*, WO2000046157, 2000.

14 J. Henschel, F. Horsthemke, Y. P. Stenzel, M. Evertz, S. Girod, C. Lürenbaum, K. Kösters, S. Wiemers-Meyer, M. Winter and S. Nowak, Lithium ion battery electrolyte degradation of field-tested electric vehicle battery cells – A comprehensive analytical study, *Journal of Power Sources*, 2020, **447**, 227370.

15 A. Šimek, T. Kazda, J. Báňa and O. Čech, Basic method for water detection in $LiPF_6$-based electrolytes, *Monatsh. Chem.*, 2024, **155**, 313–317.

16 M. D. S. Lekgoathi, B. M. Vilakazi, J. B. Wagener, J. P. Le Roux and D. Moolman, Decomposition kinetics of anhydrous and moisture exposed $LiPF_6$ salts by thermogravimetry, *Journal of Fluorine Chemistry*, 2013, **149**, 53–56.

17 T. Kawamura, S. Okada, and J. Yamaki, Decomposition reaction of $LiPF_6$-based electrolytes for lithium ion cells, *Journal of Power Sources*, 2006, **156** (2), 547–554.

18 U. Heider, R. Oesten, and M. Jungnitz, Challenge in manufacturing electrolyte solutions for lithium and lithium ion batteries quality control and minimizing contamination level, *Journal of Power Sources*, 1999, **81–82**, 119–122.

19 L. Terborg, S. Weber, F. Blaske, S. Passerini, M. Winter, U. Karst and S. Nowak, Investigation of thermal aging and hydrolysis mechanisms in commercial lithium ion battery electrolyte, *Journal of Power Sources*, 2013, **242**, 832–837.

20 V. Kraft, M. Grützke, W. Weber, M. Winter and S. Nowak, Ion chromatography electrospray ionization mass spectrometry method development and investigation of lithium hexafluorophosphate-based organic electrolytes and their thermal decomposition products, *Journal of Chromatography A*, 2014, **1354**, 92–100.

21 C. L. Campion, B. L. Lucht, R. Boris, J. DiCarlo, R. Gitzendanner, and K. M. Abraham, Abstract 58, The 224th American Chemical Society Meeting, Decomposition of carbonate solvents in solutions containing $LiPF_6$, Boston, MA, Aug 18-22, 2002.

22 A. V. Plakhotnyk, L. Ernst and R. Schmutzler, Hydrolysis in the system $LiPF_6$—propylene carbonate—dimethyl carbonate—H_2O, *Journal of Fluorine Chemistry*, 2005, **126**, 27–31.

23 K. Tasaki, K. Kanda, S. Nakamura and M. Ue, Decomposition of $LiPF_6$ and stability of PF_5 in Li-ion battery electrolytes. Density functional theory and molecular dynamics studies., *J. Electrochem. Soc.*, 2003, **150**, A1628–A1636.

24 A. E. Gebala and M. M. Jones, The acid catalyzed hydrolysis of hexafluorophosphate, *Journal of Inorganic and Nuclear Chemistry*, 1969, **31**, 771–776.

25 H. R. Clark and M. M. Jones, Ligand substitution catalysis *via* hard acid-hard base interaction, *J. Am. Chem. Soc.*, 1970, **92**, 816–822.

26 H. R. Clark and M. M. Jones, The acid and metal salt catalyzed hydrolyses of $PO_2F_2^-$ and PO_3F^{2-}, *Inorg. Chem.*, 1971, **10**, 28–33.

27 L. N. Devonshire and H. H. Rowley, Kinetics of hydrolysis of fluorophosphates. I. Monofluorophosphoric acid, *Inorg. Chem.*, 1962, **1**, 680–683.

28 J. W. Larson and B. Su, Thermodynamics of formation of aqueous monofluoro-, difluoro-, and amidofluorophosphoric acids, *J. Chem. Eng. Data*, 1994, **39**, 36–38.

29 J. D. Allison, D. S. Brown and K. J. Novo-Gradac, *MINTEQA2/PRODEFA2, a Geochemical Assessment Model for Environmental Systems: Version 3.0 User's Manual*, Environmental Research Laboratory, Office of Research and Development, U.S. Environmental Protection Agency, 1991.

30 PHREEQCE Welcome page, https://wwwbrr.cr.usgs.gov/projects/GWC_coupled/phreeqe/, (Accessed August 9, 2024).

31 M. Hirano, T. Kuga, M. Kitamura, S. Kanaya, N. Komine and S. Komiya, Acid-promoted hydrogen migration in (2-allylphenoxo)ruthenium(II) to form an η^3-Allyl complex, *Organometallics*, 2008, **27**, 3635–3638.

32 Donald R. Burgess (2004), NIST SRD 46. Critically Selected Stability Constants of Metal Complexes: Version 8.0 for Windows, National Institute of Standards and Technology, https://doi.org/10.18434/M32154 (Accessed August 9, 2024).

33 M. Meyn, K. Beneke, and G. Lagaly, Anion-exchange reactions of layered double hydroxides, *Inorg. Chem.*, 1990, **29**(26), 5201–5207.

Data availability

The data supporting this article have been included as part of the ESI. The raw data of this study are available from the corresponding authors upon request.

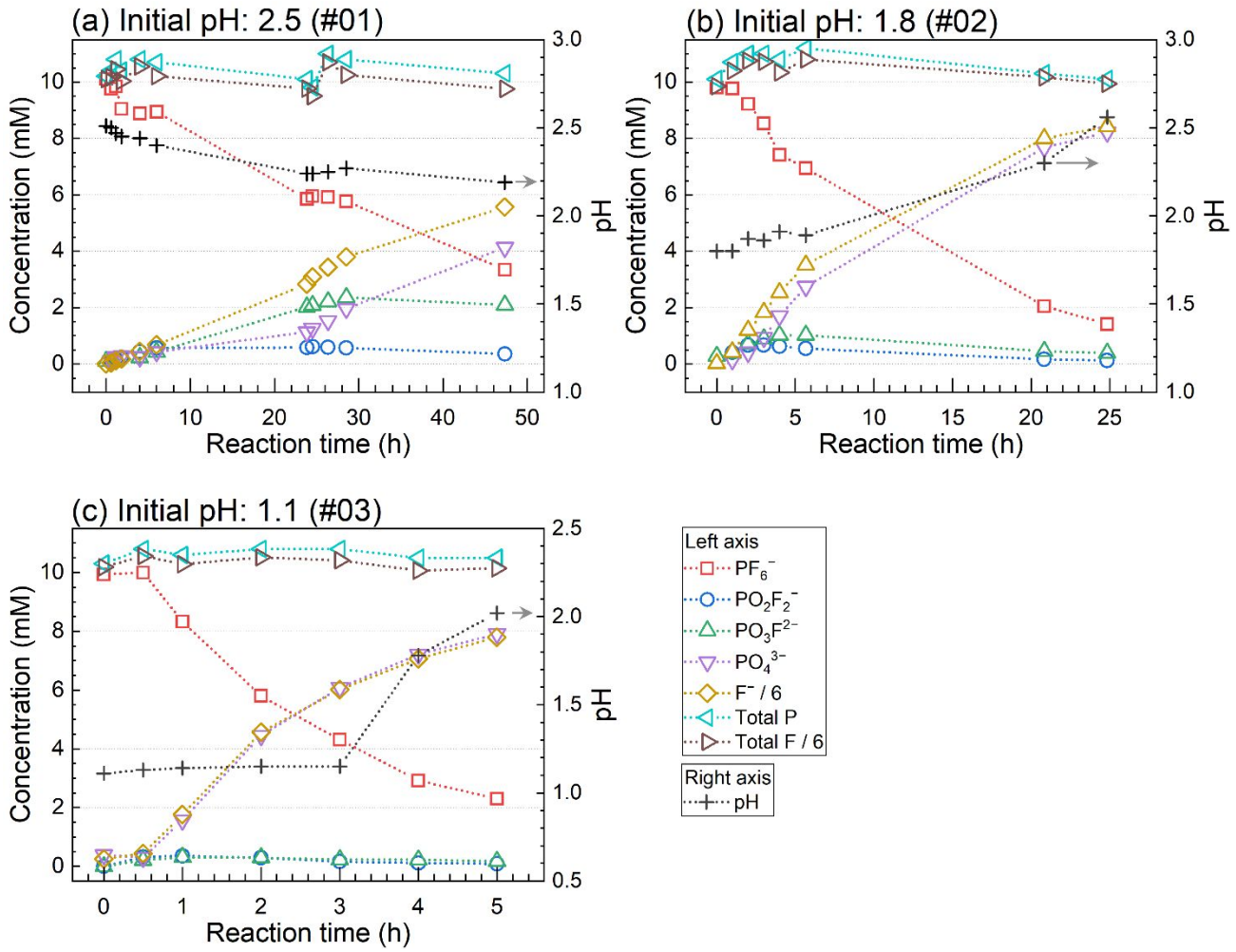

Fig. 1 Changes of pH and concentrations of PF_6^-, $PO_2F_2^-$, PO_3F^{2-}, PO_4^{3-}, and F^- when 10 mM $LiPF_6$ solutions with initial pH (a) 2.5, (b) 1.8, and (c) 1.1 were kept at 90 °C. The concentrations of anions were measured by ion chromatography. Total P and total F were calculated from the sum of each anion concentration. The measured pH values may be higher than the correct values due to the effect of HF on the pH electrode by the produced pH (see Fig. S4).

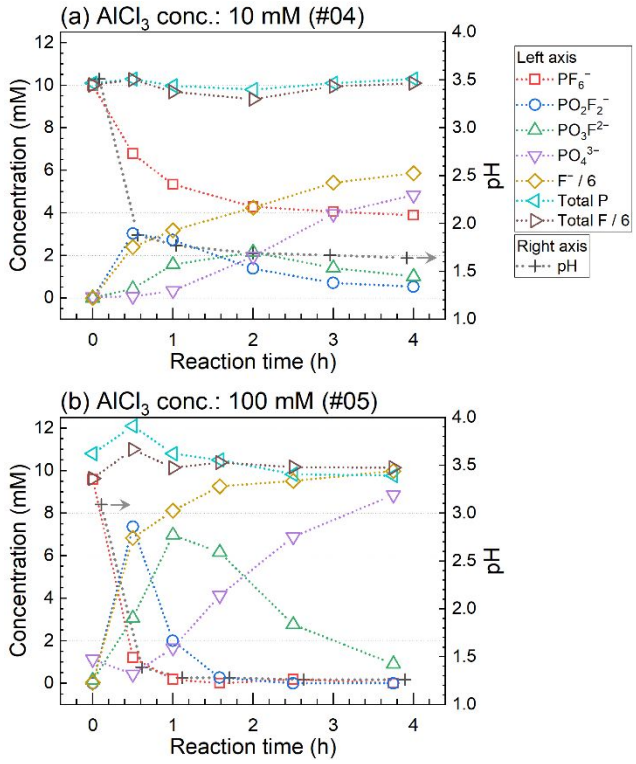

Fig. 2 Changes of pH and concentrations of PF_6^-, $PO_2F_2^-$, PO_3F^{2-}, PO_4^{3-}, and F^- when 10 mM $LiPF_6$ solutions with (a) 10 mM $AlCl_3$ and (b) 100 mM $AlCl_3$ were kept at 90 °C. The concentrations of anions were measured by ion chromatography. Total P and total F were calculated from the sum of each anion concentration.

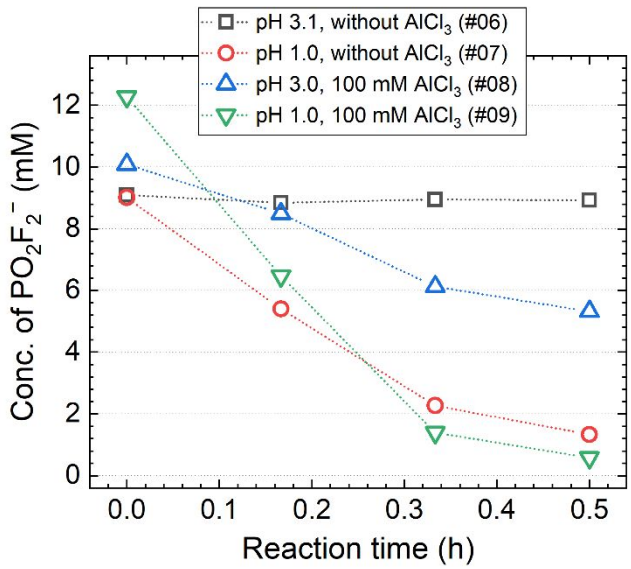

Fig. 3 Concentration changes of $PO_2F_2^-$ when 10 mM $LiPO_2F_2$ solutions with initial pH 3.1 without $AlCl_3$ (exp. #06), initial pH 1.0 without $AlCl_3$ (exp. #07), initial pH 3.0 with 100 mM $AlCl_3$ (exp. #08), and initial pH 1.0 with 100 mM $AlCl_3$ (exp. #09) were kept at 90 °C. The concentration of $PO_2F_2^-$ was measured by ion chromatography.

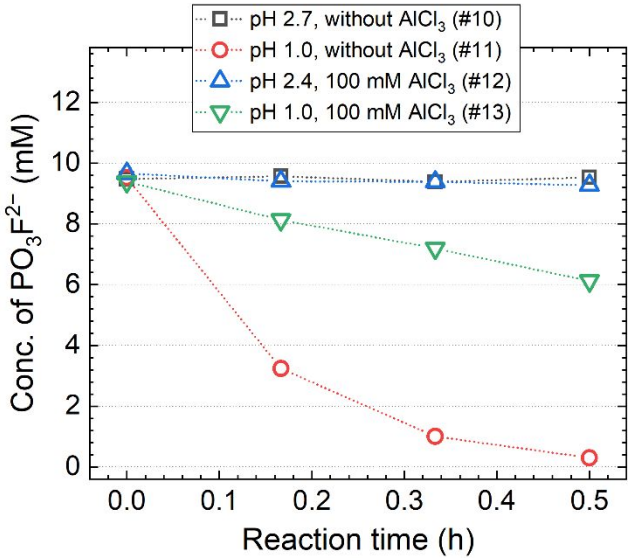

Fig. 4 Concentration changes of PO_3F^{2-} when 10 mM Na_2PO_3F solutions with initial pH 2.7 without $AlCl_3$ (exp. #10), initial pH 1.0 without $AlCl_3$ (exp. #11), initial pH 2.4 and 100 mM $AlCl_3$ (exp. #12), and initial pH 1.0 and 100 mM $AlCl_3$ (exp. #13) were kept at 90 °C. The concentration of PO_3F^{2-} was measured by ion chromatography.

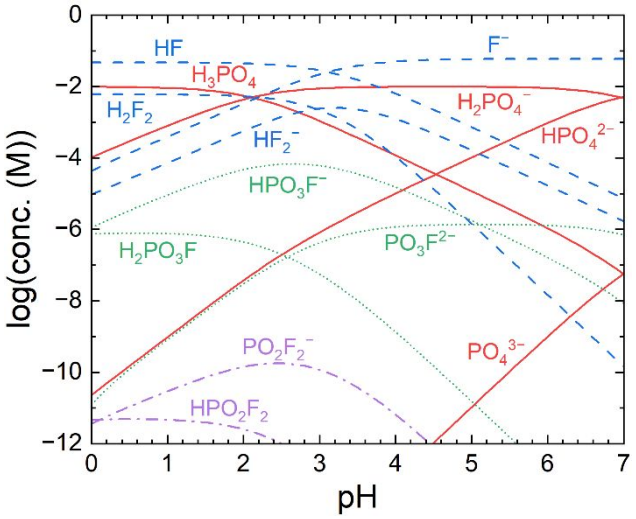

Fig. 5 Equilibrium concentrations of each chemical species for the P-F system in aqueous solution calculated by PHREEQC version 2 at the Initial concentration of 10 mM PO_4^{3-} and 60 mM F^-.

Table 1 Acid dissociation constant (pK_a) for each acid.

Molecular formula	**HPF_6**	**HPO_2F_2**	**H_2PO_3F**	**H_3PO_4**	**HF**
Acidity constant	$pK_a = -20$*	$pK_a = 0.298$	$pK_{a1} = 0.0175$ $pK_{a2} = 5.331$	$pK_{a1} = 2.148$ $pK_{a2} = 7.198$ $pK_{a3} = 12.375$	$pK_a = 3.17$
Ref.	Hirano *et al.*[31]	Larson and Su[28]	Larson and Su[28]	minteq.v4.dat[29]	minteq.v4.dat[29]

*Original data was not given in ref. 31.

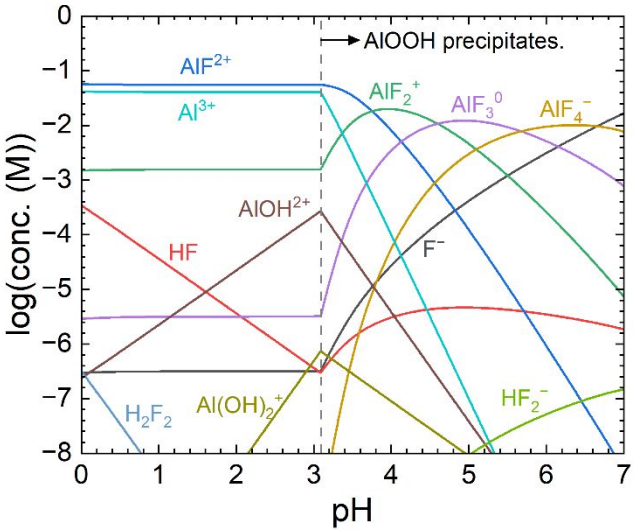

Fig. 6 Equilibrium concentrations of each chemical species for the Al-F system in aqueous solution calculated by PHREEQC version 2 at the initial concentration of 100 mM Al^{3+} and 60 mM F^-.

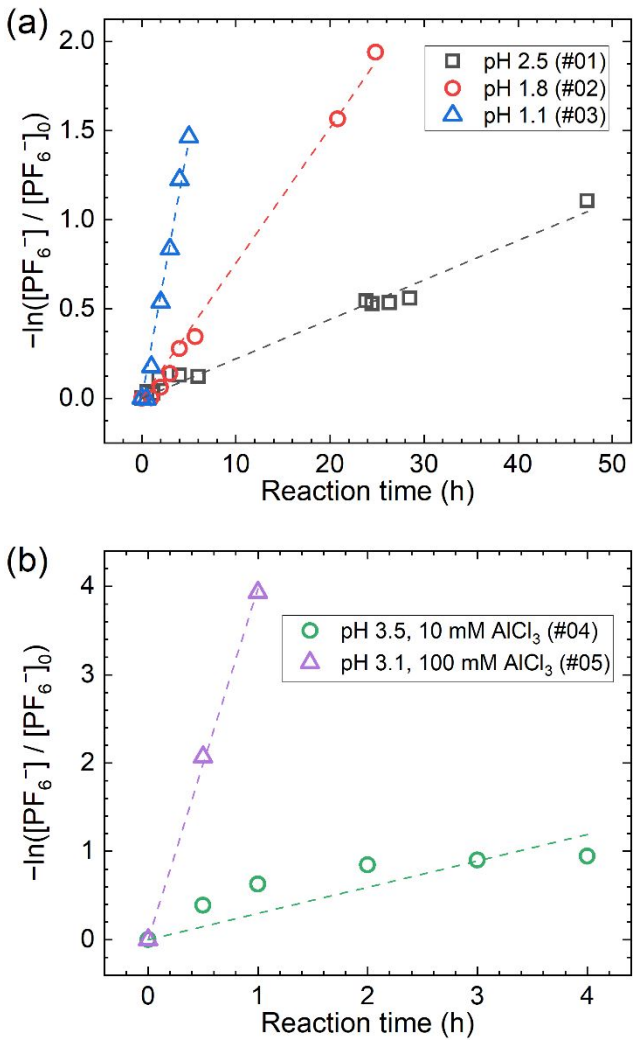

Fig. 7 The values of $-\ln\left(\frac{[PF_6^-]}{[PF_6^-]_0}\right)$ plotted against reaction time t in exp. (a) #01–03 and (b) #04–05. The dashed lines are the fitted lines by the least-squares method through the origin.

Table 2 Pseudo-first-order reaction rate constant (k_{obs}) for hydrolysis of PF_6^- obtained in this work.

Exp. no.	PF_6^- Conc. (mM)	Initial pH	$AlCl_3$ conc. (mM)	Temperature (°C)	Number of plots	k_{obs}* ($\times 10^{-4}$ min^{-1})
#01	10	2.5	0	90	11	3.68 ±0.10
#02		1.8			8	12.6 ±0.34
#03		1.1			7	48.2 ±1.9
#04		3.5	10		6	49.6 ±7.3
#05		3.1	100		3	662 ±9.8

*Calculated using the least-squares method through the origin, and ± denotes standard error.

Table 3 Pseudo-first-order reaction rate constant (k_{obs}) for hydrolysis of (a) PF_6^-, (b) $PO_2F_2^-$, and (c) PO_3F^{2-} reported in previous works.

(a)

PF_6^- Conc. (mM)	HCl conc. or pH	Added cation	Temperature (°C)	k_{obs} ($\times 10^{-4}$ min^{-1})	Ref.
1	1.0 M	None	25	0.0764	Clark and Jones[25]
		10 mM Zr^{4+}	25	3.98	
		10 mM Th^{4+}		3.19	
		10 mM Al^{3+}		0.451	
	2.0 M	None	45	3.98	Gebala and Jones[24]
			35	0.940	
			25	0.214	
		10 mM Zr^{4+}		16.1	Clark and Jones[25]
		10 mM Th^{4+}		3.92	
		10 mM Al^{3+}		0.745	

(b)

$PO_2F_2^-$ Conc. (mM)	HCl conc. or pH	Added cation	Temperature (°C)	k_{obs} ($\times 10^{-4}$ min^{-1})	Ref.
2	1.0 M	None	35	7.11	Clark and Jones[26]
			25	3.25	
	2.0 M			9.83	
	pH 2	200 mM Al^{3+}	25	0.011	
		400 mM Al^{3+}		0.028	
		600 mM Al^{3+}		0.037	
		800 mM Al^{3+}		0.053	
		1000 mM Al^{3+}		0.065	

(c)

PO_3F^{2-} Conc. (mM)	HCl conc. or pH	Added cation	Temperature (°C)	k_{obs} ($\times 10^{-4}$ min^{-1})	Ref.
4	1.0 M	None	35	14.4	Clark and Jones[26]
			25	6.0	
		5 mM Zr^{4+}	25	0.68	
	2.0 M	None	25	15.0	

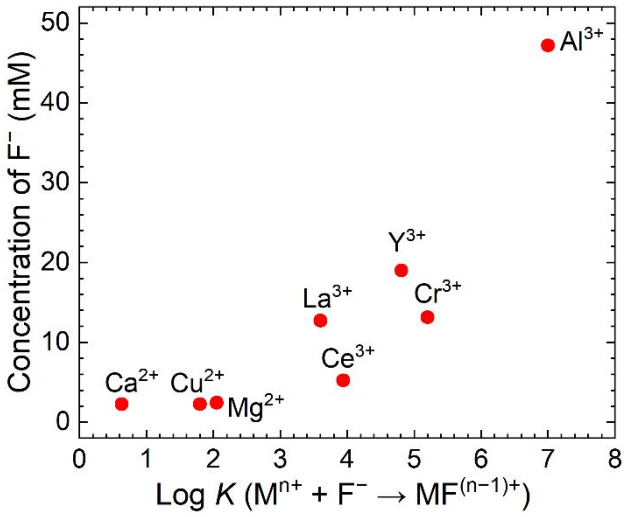

Fig. 8 Relationship between the formation constant (log *K*) of fluoride complex for each cation ($M^{n+} + F^- \rightarrow MF^{(n-1)+}$) and the concentrations of F^- when 10 mM $LiPF_6$ solutions with various cations (2 mM) at initial pH 3.8–4.0 were kept at 90 °C for 24 hours. The value of log *K* was obtained from the NIST SRD 46 database (The ionic strength of is 0 except for Ca^{2+} and 1 for Ca^{2+}).[32]

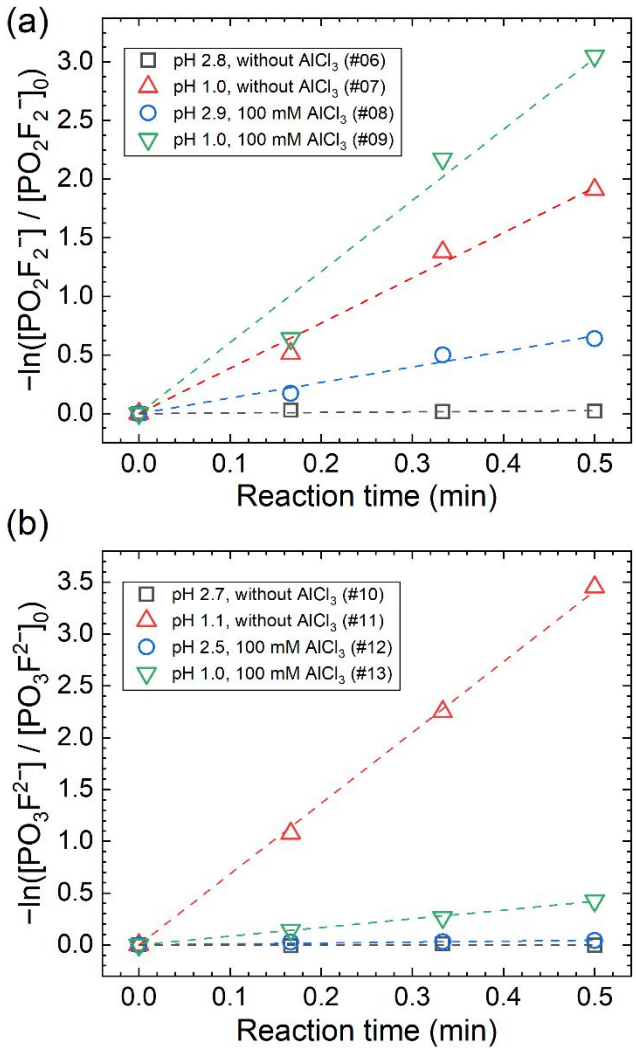

Fig. 9 The values of (a) $-\ln\left(\frac{[PO_2F_2^-]}{[PO_2F_2^-]_0}\right)$ in exp. 06–09 and (b) $-\ln\left(\frac{[PO_3F^{2-}]}{[PO_3F^{2-}]_0}\right)$ in exp. 10–13 plotted against reaction time t.

Table 4 Pseudo-first-order reaction rate constant (k_{obs}) for hydrolysis of (a) $PO_2F_2^-$ and (b) PO_3F^{2-} obtained in this work.

(a)

Exp. no.	$PO_2F_2^-$ Conc. (mM)	Initial pH	$AlCl_3$ conc. (mM)	Temperature (°C)	Number of plots	k_{obs} ($\times10^{-4}$ min^{-1})
#06	10	3.1	0	90	4	8.23±3.2
#07		1.0			4	643 ±25
#08		3.0	100		4	221 ±12
#09		1.0			4	1010 ±62

(b)

Exp. no.	PO_3F^{2-} Conc. (mM)	Initial pH	$AlCl_3$ conc. (mM)	Temperature (°C)	Number of plots	k_{obs} ($\times10^{-4}$ min^{-1})
#10	10	2.7	0	90	4	−0.438±2.3
#11		1.0			4	1140 ±12
#12		2.4	100		4	14.9 ±1.9
#13		1.0			4	140 ±2.4

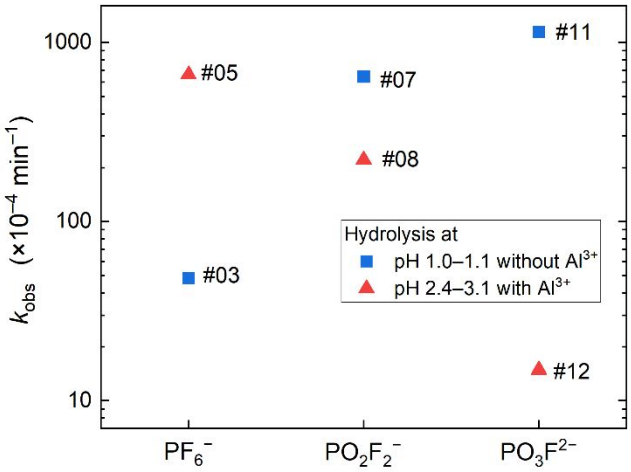

Fig. 10 Pseudo-first-order reaction rate constant (k_{obs}) plotted against PF_6^-, $PO_2F_2^-$, and PO_3F^{2-} for the hydrolysis at pH 1.0–1.1 without Al^{3+} (exp. #03, #07, and #11) and at pH 2.4–3.1 with 100 mM Al^{3+} (exp. #05, #08, and #12).

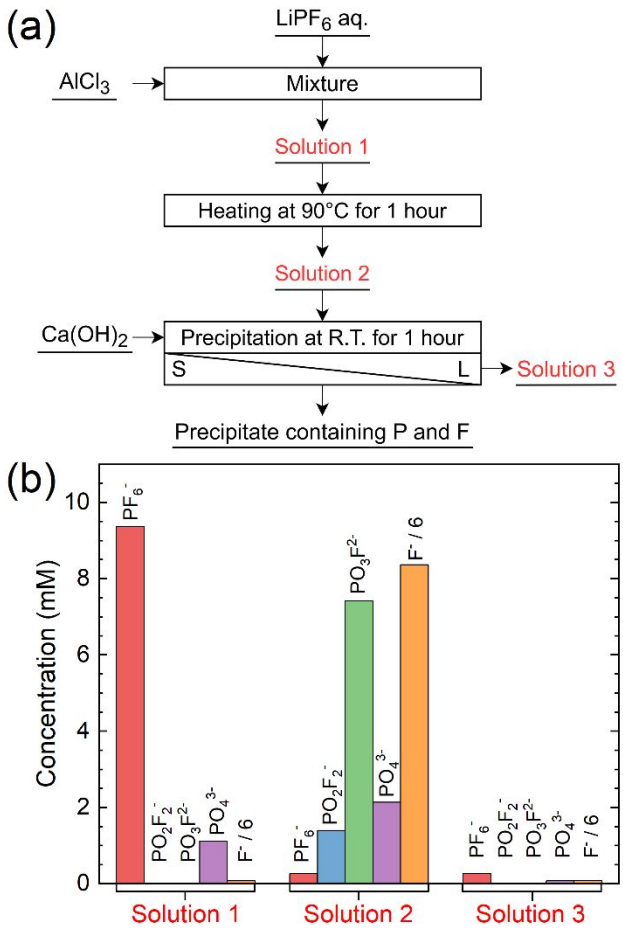

Fig. 11 (a) Flowchart of the process for more efficient treatment proposed in this study. (b) The concentration of PF_6^-, $PO_2F_2^-$, PO_3F^{2-}, PO_4^{3-}, and F^- measured by ion chromatography for the solutions prepared with 10 mM $LiPF_6$ and 100 mM $AlCl_3$ (solution 1), kept at 90 °C for 1 hour (solution 2), and then mixed with 432 mM $Ca(OH)_2$ at room temperature for 1 hour (solution 3).